World Journal of Advanced Engineering Technology and Sciences
eISSN: 2582-8266
Cross Ref DOI: 10.30574/wjaets
Journal homepage: https://wjaets.com/

(RESEARCH ARTICLE)

Check for updates

Soil erosion hazard assessment using the RUSLE model for the Taung Watershed of Ramotswa Agricultural District in Botswana

Motshereganyi Sylvester Moesi, Benedict Kayombo *, Rejoice Tsheko and Emmanuel Setlhabi

Department of Agricultural and Biosystems Engineering, Botswana University of Agriculture and Natural Resources, Private Bag 0027, Gaborone, Botswana.

World Journal of Advanced Engineering Technology and Sciences, 2023, 09(01), 029–041

Publication history: Received on 19 March 2023; revised on 03 May 2023; accepted on 06 May 2023

Article DOI: https://doi.org/10.30574/wjaets.2023.9.1.0129

Abstract

The Revised Universal Soil Loss Equation (RUSLE) model integrated with Remote Sensing (RS) and Geographical Information Systems (GIS) was positively validated to spatially assess soil erosion risk in the Taung Watershed of Ramotswa Agricultural District during the period 2000 – 2020. The estimated annual soil erosion averaged 12.04 and 12.74 t/ha/year in 2000 and 2020, respectively. The Land Use/Land Cover (LULC) and soil type were found to be key determinants of high soil erosion hazard when using RUSLE. The soil erosion assessment tools enabled prioritization of high erosion prone areas in the study area for soil conservation planning and watershed management.

Keywords: Taung watershed; Soil erosion hazard; RUSLE; RS; GIS

1. Introduction

Soil erosion has become a major component in the overall environmental degradation in the world that threatens food production [1]. Soil erosion can be accelerated by anthropogenic activities such as excessive cutting of trees, overgrazing [2] and tillage operations [3]. According to Pimentel and Burgess [4], about 10 million ha of arable land is dissipated due to soil erosion hence reducing the arable land that is available for world food production. About 16% of the land in Africa is degraded and soil erosion is of great concern in Sub- Saharan African countries [5]. Botswana, located in semi-arid environments, is most vulnerable to soil erosion threats due to less biomass to sustain soil structural integrity [6].

Population explosion, deforestation, unsustainable agricultural cultivation, and overgrazing are among the main factors causing soil erosion hazards in the highly degraded Kweneng, Kgatleng and Southern Districts of Botswana [7].

To select suitable conservation actions, the identification and quantification of soil loss sources are necessary [8]. Generally, soil erosion can be assessed using different soil erosion models which vary in degrees of complexity [9]. Soil erosion empirical models have proved to be the cheaper way of assessing the distribution and magnitude of erosion in watershed areas in Southern Africa [10]. The most widely applied empirical soil loss models are the Revised Universal Soil Loss Equation (RUSLE) and Soil Loss Estimation Model for Southern Africa (SLEMSA).

The introduction of Geographical Information Systems (GIS) and Remote Sensing (RS) technology has made it possible to implement the equation in a spatially distributed manner and prediction of soil erosion on a cell-by-cell basis [11]. It has several advantages in terms of identifying areas that are highly capable of being physically degraded, quantifying rates of soil loss, and mapping erosion prone areas [12].

* Corresponding author: Benedict Kayombo

Very little is currently known about the assessment and mapping of high erosion prone areas in the Southern District including South East of Botswana. The livelihood of the people in the Ramotswa Agricultural District of South East Botswana relies on crop and animal production. Soil erosion and soil fertility decline are accelerated by anthropogenic activities including use of crop residues as animal feed. It is vital to have information on the distribution patterns of soil loss hazard areas and their severity as it can be used for soil conservation planning. It is imperative to reduce soil erosion to raise agricultural productivity in the study area. The objective of the present study was, therefore, to assess the soil erosion hazard in the Taung Watershed of Ramotswa Agricultural District using the RUSLE model integrated with RS-GIS.

2. Material and methods

2.1. Description of study area

The Taung Watershed is in Ramotswa Agricultural District and covers about 43 958 ha. It extends from 24° 50' 0''- 25 50' 0'S latitude and 25° 35' 0''- 25 50' 0'' E longitude. The climate is semiarid. The rainfall is seasonal, with the wet season normally occurring between October and March while dry and cold winter months range from May to July. The mean total annual rainfall ranges from 400 to 550 mm. High temperatures are experienced during the wet season, recording between 30 to 32 °C on average during the day and between 16 to 20 °C on average at night. The watershed has a highly uneven elevation ranging from 1012 to 1489 m above sea level. The soils range from fine sands - loamy Fine sand to Sandy Loams - Sandy Clay. The vegetation cover within the watershed is predominantly mixed shrub savannah and tree savannah [13]. An overview of the boundary of the study area is given in Figure 1.

2.2. Mapping of soil erosion hazard

Mapping of soil erosion hazard in the study area was carried out according to RUSLE model (Equation 1).

$$A = R*K*LS*C*P \quad \ldots\ldots (1)$$

Where A is the mean annual soil loss rate (t/ha/year); R is rainfall erosivity factor (MJ/mm/ha/year); K is the soil erodibility factor (t/ha/MJ/mm); LS is slope length and slope steepness factor (dimensionless); C = cover management factor (dimensionless); and P is erosion control practice factor (dimensionless).

2.2.1. Rainfall erosivity factor (R)

Long-time annual rainfall point data for a period of 26 years from 7 stations in and around Taung Watershed was obtained from the Department of Meteorological Services. Rainfall energy was then determined according to Equation (2) for erosive rainfall. The mean annual rainfall was first interpolated to generate continuous rainfall data for each grid cell by using Analyst Tools Raster Inverse Distance Weighting (IDW) Interpolation in ArcGIS to create a raster map for the area. Details of the rainfall stations are presented in Table 1.

$$R = 0.5*P \quad \ldots\ldots (2)$$

Where, R is rainfall erosivity and P is the mean annual precipitation (mm).

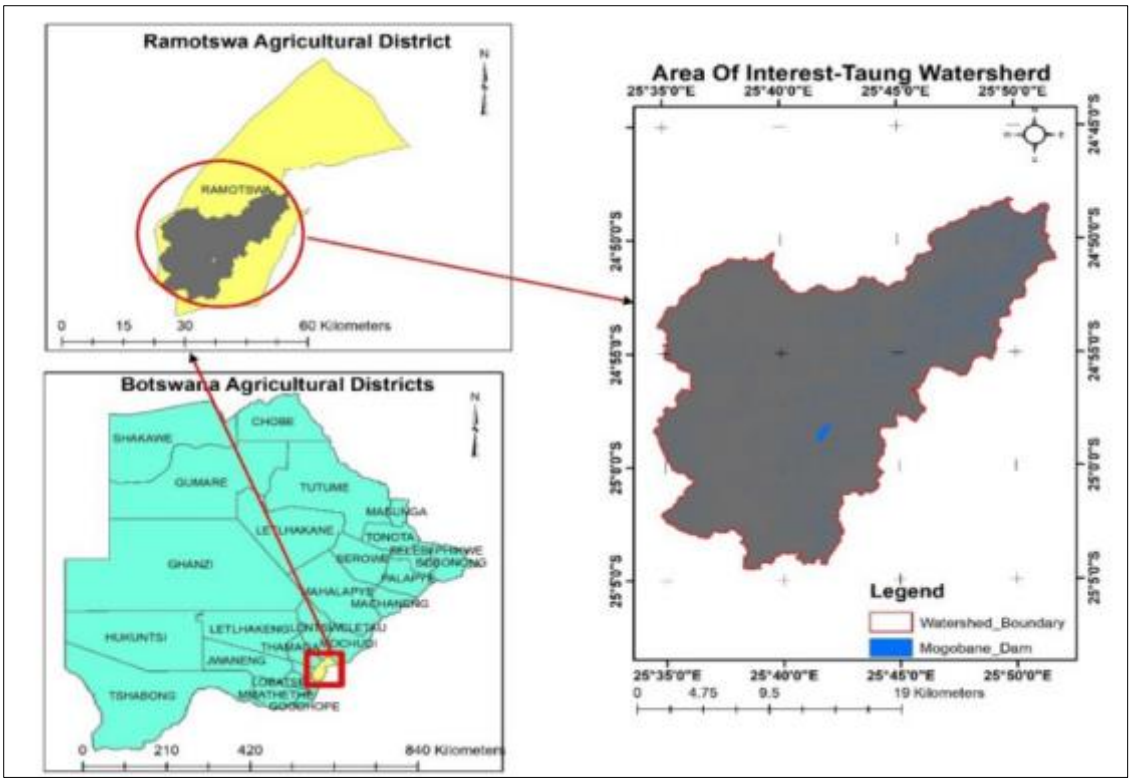

Figure 1 Location of Taung Watershed in Ramotswa Agricultural District of Southern District, Botswana

Table 1 Mean annual rainfall of meteorological stations in the study area

Weather Stations No	Rainfall Weather Stations	Years of Observation	Mean Annual Rainfall (MAR) in mm	Northings	Eastings
1	Seepapitso-Kanye	1990-2015	453	-24.93333	25.36667
2	Moshupa Police Station	1990-2015	510	-24.76667	25.43333
3	Mogobane	1991, 1992, 1993, 1997, 2001 and 2005	480	-24.95000	25.700000
4	Ramotswa Station	1971-2014	483	-24.88333	25.86667
5	Gaborone MET H. Q	1989-2015	498	-24.66667	25.91667
6	Moeding College	1995-2019	505	-25.01667	25.73333
7	Lobatse Police Station	1999-2015	488	-25.25000	25.65000

2.2.2. Soil erodibility factor (K)

The Digital Soil Map obtained from the Ministry of Agricultural Development and Food Security was used to derive K factor values for the study area according to Roose [14] as shown in Table 2.

Table 2 Soil erodibility factor (K) according to soil texture

Textural Class	**Organic Matter Content**		
	<0.5%	**2%**	**4%**
Sand	0.05	0.03	0.02
Fine sand	0.16	0.14	0.10
Very fine sand	0.42	0.36	0.28
Loamy sand	0.24	0.20	0.16
Loam very fine sand	0.44	0.38	0.30
Sandy loam	0.27	0.24	0.19
Fine sandy loam	0.35	0.30	0.24
Loam	0.47	0.41	0.33
Silt loam	0.38	0.34	0.29
Silt	0.48	0.42	0.33
Sandy clay loam	0.60	0.52	0.42
Clay loam	0.27	0.25	0.21
Silty clay loam	0.28	0.25	0.21
Sandy clay	0.37	0.32	0.26
Silty clay	0.14	0.13	0.12
Clay	0.25	0.23	0.19

Source: Roose [14]

2.2.3. Slope length and slope steepness (LS)

The Shuttle Radar Topography Mission (SRTM) Digital Elevation Model (DEM) of spatial resolution of 90 m was used to generate the LS factor. The DEM was filled to generate a depression-free DEM using the fill sink tool. The flow directions were then computed from the flow direction toolset. From the flow direction, flow accumulation was derived. The slope and flow accumulation were used to calculate the LS factor using the Raster Calculator in ArcMap 10.7 according to Equation (3) derived by Bizuwerk et al. [15]. The map was resampled to a 30 m cell size.

$$LS = \sqrt{(X/22.1)}\ m\ (0.065+0.045s+0.0065s^2) \quad \ldots\ldots\ldots\ldots\ldots\ldots \ (3)$$

Where X = Flow accumulation*cell size and cell size is the resolution of the grid (i.e., 90 m), s = Slope gradient (%), and m is a slope contingent variable.

2.2.4. Cover management factor (C)

The LULC map for 2000 and 2020 with a 30 m resolution was created with a maximum likelihood supervised classification of five different LULC classes (vis. Cultivated land, Shrubland, Built-up areas, Woodland, and Waterbody) using Geomatica 2018. After the classification, the raster layer was converted into a vector layer and the C-factor values were assigned for each LULC class accordingly (Table 3). The C values were then converted to raster by conversion tool method from polygon.

2.2.5. Erosion control practice factor (P)

The P factor was derived from the LULC maps according to how various authors assigned P-values to different LULC classes (Table 4).

2.2.5. Soil erosion hazard analysis

The six RUSLE factors (R,K,LS,C and P) were all converted into a raster format and each layer was then changed to the same cell size of 30 m. Layers were overlaid/multiplied through the use of the Raster Calculator toolset in ArcMap 10.7. The results of those factors were recorded as the soil erosion hazard of the study area in tons/ha/year for the years 2000 and 2020. The R, K and LS were assumed to be the same for years 2000 and 2020 while the C and P factors varied.

The soil erosion hazard was then categorized into different severity classes to determine erosion hazard priority areas for conservation planning [22].

2.3. Software Packages and Data Processing

Geomatica 2018 Catalyst Professional software was used for image processing and digital image classification or spectral class recognition was accomplished by supervised classification. The classification results (i.e. land cover raster image) were exported into ArcMap 10.7 for accuracy assessment with the aid of high-resolution imagery software, Google Earth and Google Earth Pro. Layers were spatially organized with the same resolution and coordinate system within ArcGIS environment [23]. Microsoft Office was used for presentation, documentation and pre-processing calculations in excel environment. The GeoConverter-Geoplaner software package was used for converting geographical coordinates.

2.4. Validation of RUSLE erosion model

A method of soil erosion hazard accuracy assessment by Phinzi [24] was adopted to ascertain the quality and reliability of the model's results. Kappa coefficient was used to validate the model's result in terms of eroded and non-eroded areas. The soil erosion hazard was reclassified into high and low soil erosion hazard classes from the different soil erosion hazard severity classes. After the reclassification of the soil erosion hazard maps, 10 random points were generated and loaded into a handheld GPS. The GPS was then used to locate and verify these points on the ground.

A simplified flow chart of the data analysis is shown in Figure 2.

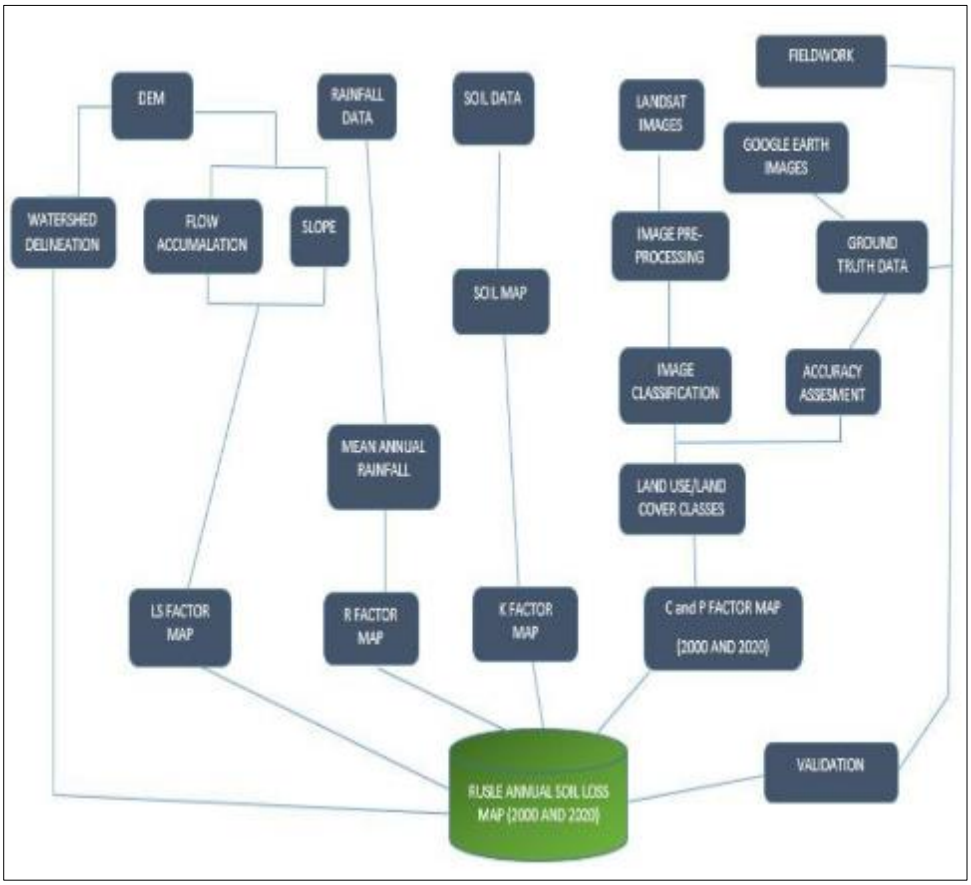

Figure 2 Flowchart for implementation of RUSLE model

3. Results and discussion

3.1. Mapping of soil erosion hazard

Mapping of soil erosion hazard in the study area was carried out according to RUSLE model. The RUSLE model includes topographic indices derived from the DEM, climatic factors, cover and soil characteristics.

3.1.1. Rainfall erosivity (R)

The mean annual precipitation data interpolated over the entire study area using IDW interpolation technique was converted to rainfall erosivity by applying Equation (2). The annual rainfall of Taung Watershed ranges from 480 to 505 mm resulting in rainfall and erosivity variation shown in Figure 3.

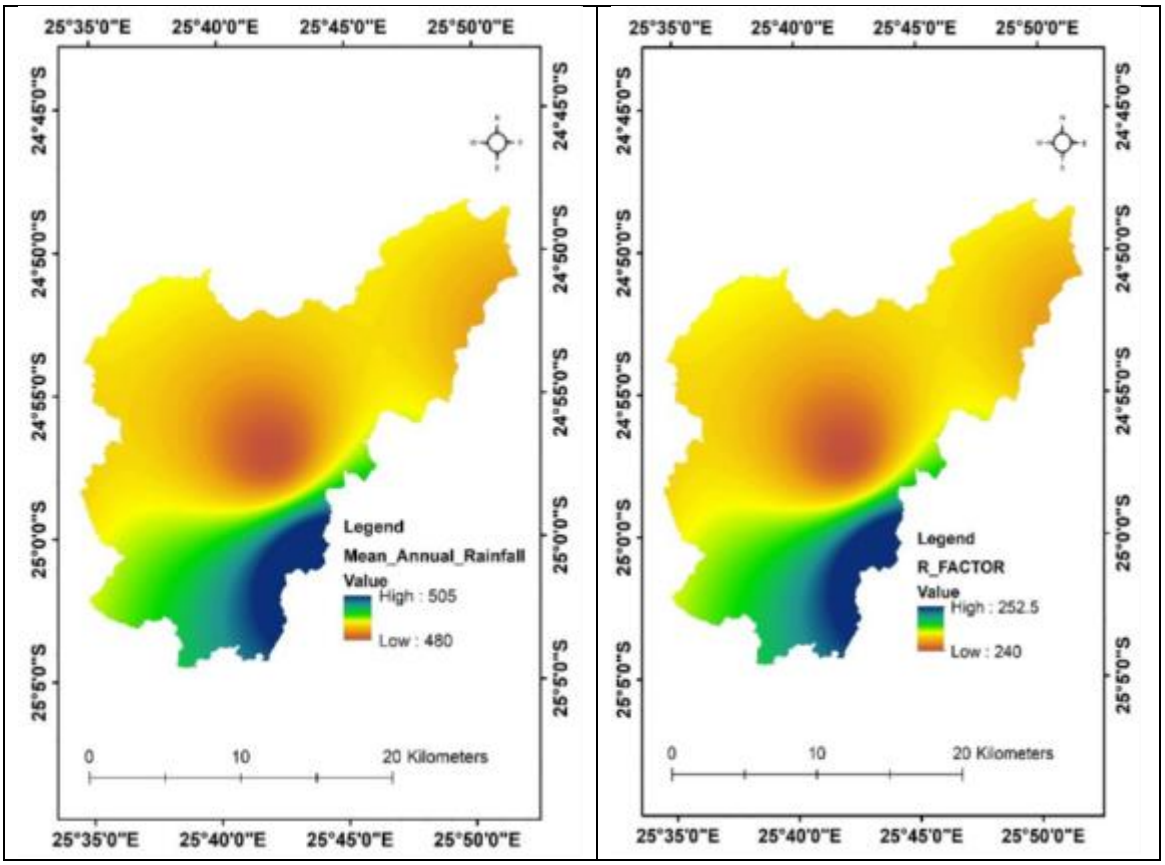

Figure 3 Rainfall and erosivity variation in Taung Watershed

3.1.2. Soil erodibility (K)

The values indicate that Fine sands to loamy fine sands and Loam sands to clay loam have lower erodibility, whereas sandy loams to clay loam and sandy loam to sandy clay had relatively medium erodibility and Sandy clay loam to sandy clay higher erodibility (Figure 4a). The results showed that the K factor value in the watershed varies from 0.026340 t/ha/MJ/mm to 0.063875 t/ha/MJ/mm (Figure 4b). The highest erodibility values were in the central, northern and southwestern parts of the watershed.

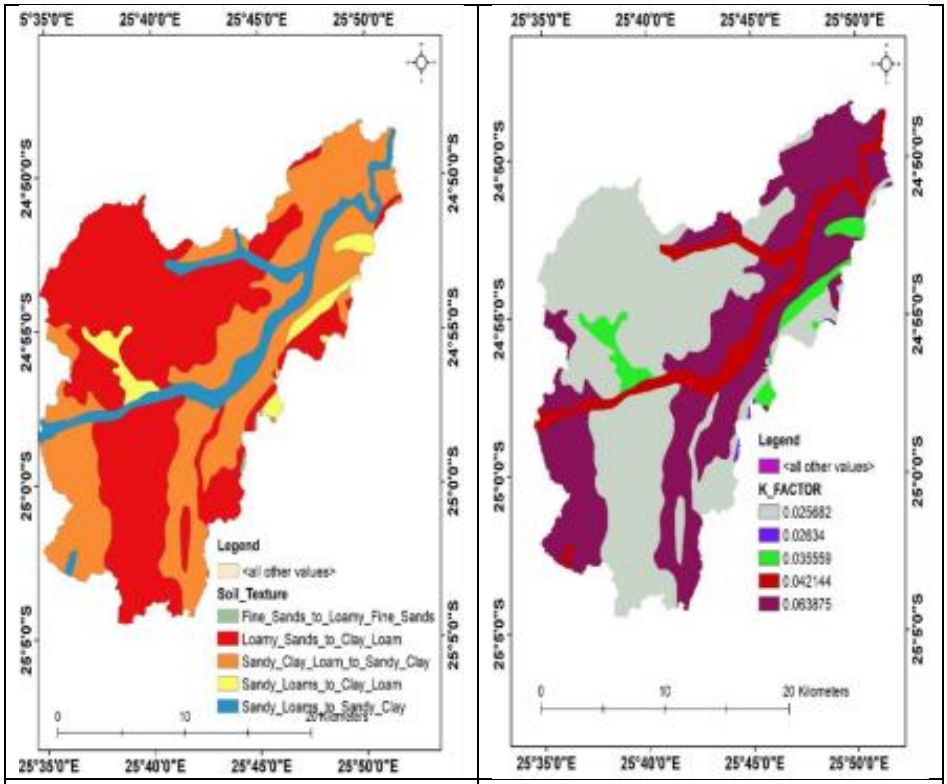

Figure 4 Soil texture (a) and associated K factor (b) maps of Taung Watershed

3.1.3. Slope length and slope steepness (LS)

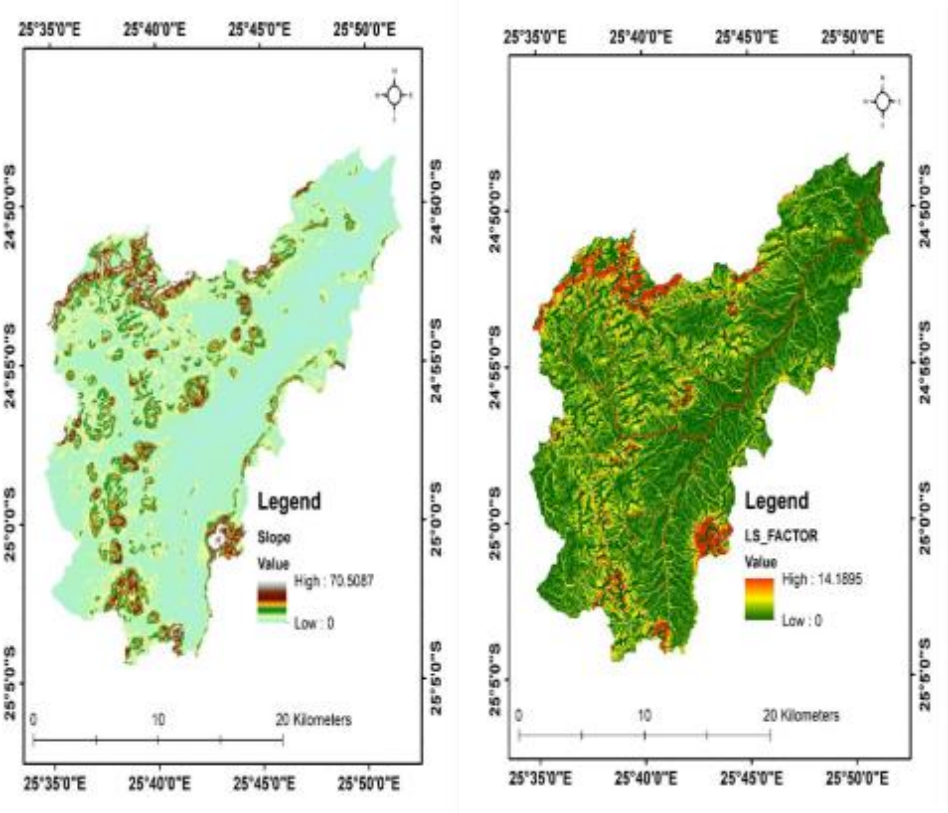

Figure 5 Slope (a) and LS factor (b) maps of Taung Watershed

The slope (in degrees) and the LS factor are shown in Figure 5. The slope varied from 0 to 70.5087 degrees (Figure 5a) whereas the LS factor ranged from 0 to 14.1895 (Figure 5b).

3.1.4. Cover management factor (C)

The LULC maps of the watershed for 2000 and 2020 (Figure 6) were used to find the C values corresponding to each land cover class. The corresponding C values for each land cover class were sourced from other studies as given in Table 3. The C values ranged from 0 to 0.2 as shown in Figure 7.

Table 3 RUSLE C factor of the study area

No	LULC	C-value	Source
1	Built-up	0.01	[19]
2	Cultivated land	0.2	[16, 19]
3	Shrubland	0.1	[16, 21]
4	Woodland (Tree Savanna)	0.001	[16, 21]
5	Waterbody	0	[16, 21]

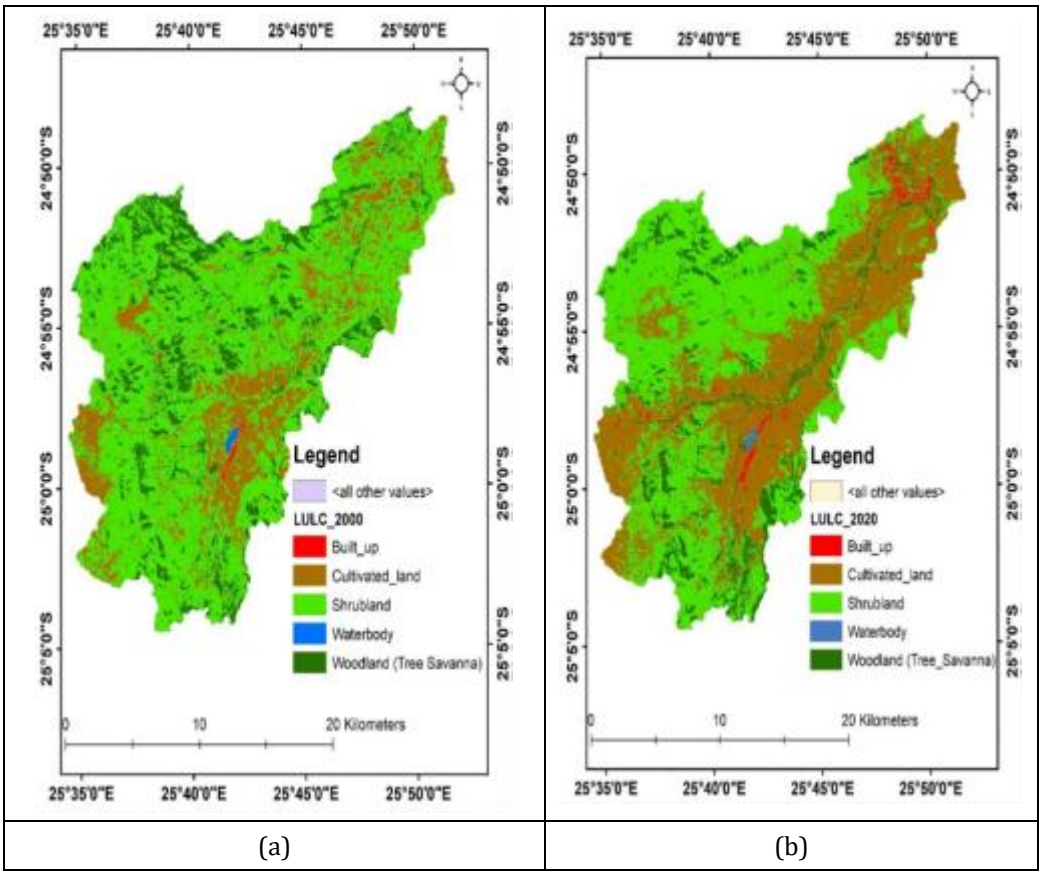

(a) (b)

Figure 6 The LULC maps of 2000 (a) and 2020 (b) for Taung Watershed

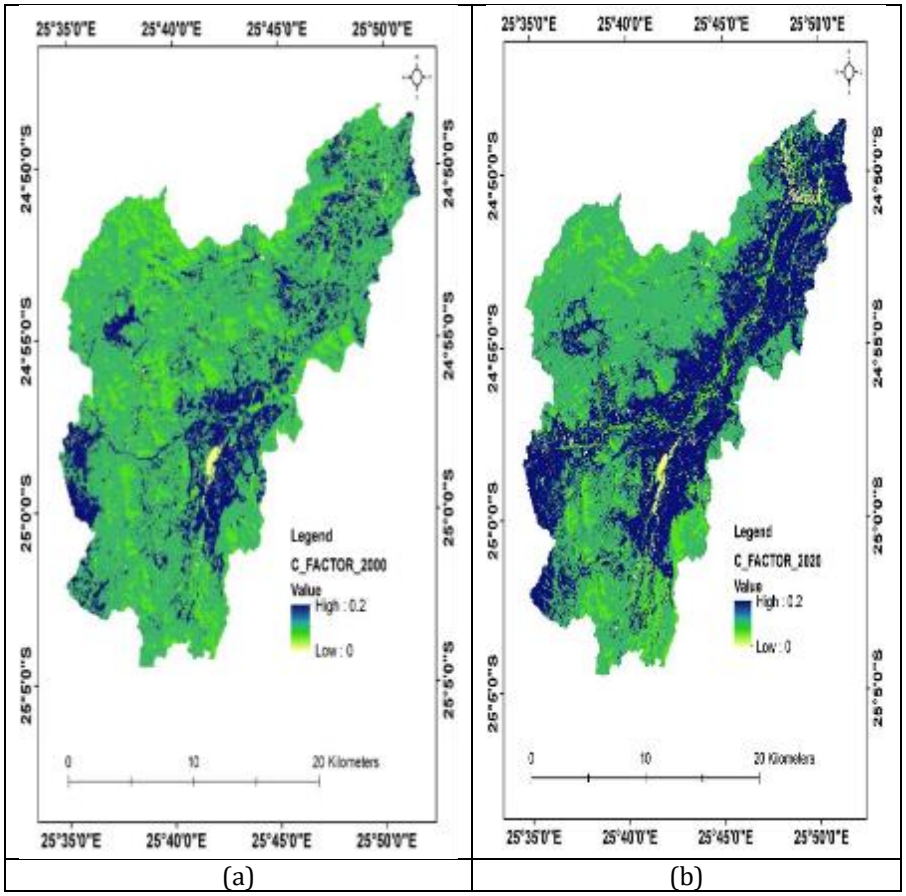

(a) (b)

Figure 7 The C factor maps of 2000 (a) and 2020 (b) for Taung Watershed

3.1.5. Management practice factor (P)

The P-values were derived from the literature varying from 0 to 0.9 across different LULC classes (Table 4). The map outputs for the P factor in 2000 and 2020 are shown in Figure 8.

Table 4 P factor of the study area

No	LULC	P-value	Source
1	Built-up	0.63	[19]
2	Cultivated land	0.90	[16, 19]
3	Shrubland	0.63	[16, 21]
4	Woodland (Tree Savanna)	0.53	[16, 21]
5	Waterbody	0	[16, 21]

The pronounced extent of the area with a high P-factor value in 2020 compared to 2000 is an obvious indication of the increased soil erosion hazard in only 20 years (Figure 8b).

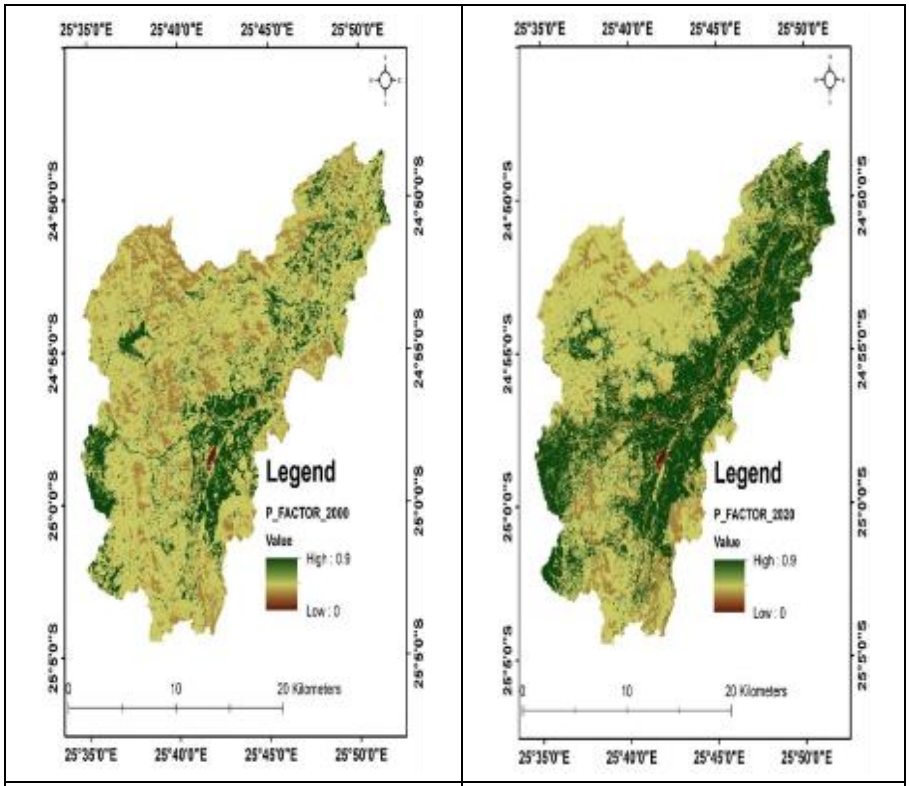

(a) (b)

Figure 8 Management practice (P) factor maps for 2000 (a) and 2020 (b)

3.2. Determination of RUSLE model

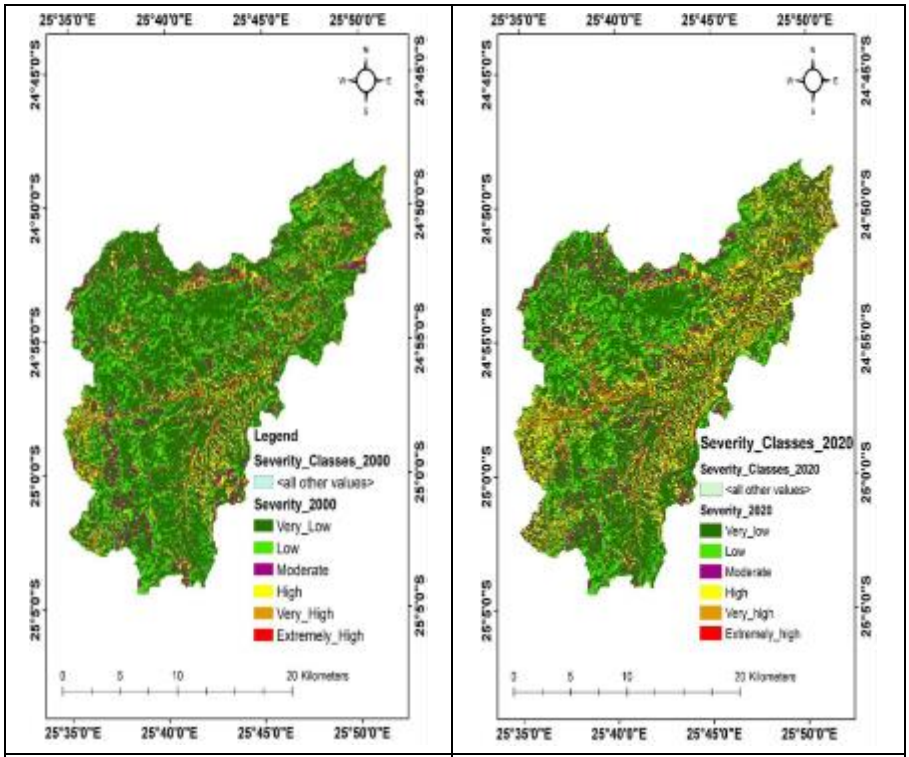

(a) (b)

Figure 9 RUSLE soil erosion severity maps of 2000 (a) and 2020 (b) for Taung Watershed

The calculation of soil erosion hazard in this model was carried out through equation A = RKLSCP to obtain the soil erosion hazard maps of 2000 and 2020 shown in Figure 9. The results were then used to determine different categories of erosion-hazard areas shown in Table 5 and Figure 9.

Table 5 RUSLE soil erosion severity in 2000-2020 for Taung Watershed

Annual Soil Loss (tons/ha/year)	Severity Classes	Priority Class	2000		2020	
			Area (ha)	Area (%)	Area (ha)	Area (%)
0-5	Very low	5	25502.12	58.01	22939.04	52.18
5-12	Low	4	8509.56	19.36	7616.4	17.33
12-25	Moderate	1	4691.83	10.67	4897.72	11.14
25-60	High	1	3000.79	6.83	5314.97	12.09
60-150	Very High	2	1755.66	3.99	2519.87	5.73
>150	Extremely High	3	498.11	1.13	670.07	1.52

Whereas the area under very low (0 – 5 t/ha/year) and low (5 – 12 t/ha/year) soil erosion hazard decreased moderately in 2020 compared to 2000, areas susceptible to moderate (12 – 25 t/ha/year) and high (25 – 60 t/ha/year) erosion hazard increased markedly in 2020 (Table 5). The area under very high (60 – 150 t/ha/year) and extremely high (>150 t/ha/year) erosion hazard also increased in 2020 compared to 2000 although the area covered was small. The model validation recorded a good agreement (Kappa = 0.78) and an overall accuracy of 90%. The RUSLE model appears to be a better soil erosion hazard predictor than SLEMSA in the study area [25].

These pronounced changes in erosion-risk severity were driven by a major increase in cultivated land and built-up area coverage while other LULC categories such as shrubland and woodland decreased during the period. This is confirmed by Matlhodi et al. [26] in the Gaborone Catchment, which covered the Taung watershed.

It is imperative, therefore, that soil conservation efforts be directed to moderate, high, very high, extremely high, low and very low erosion-risk areas, in that order of priority (Table 5).

4. Conclusion

The objective of the present study was to assess the soil erosion hazard in the Taung Watershed of Ramotswa Agricultural District using the RUSLE model integrated with RS-GIS. The model estimated the mean annual soil erosion hazard of 12.04 and 12.74 t/ha/year in 2000 and 2020, respectively. The soil type and LULC markedly contributed to a high soil erosion hazard. Most of the area in the watershed was converted into croplands from 2000 to 2020, and that accelerated the susceptibility of soil to erosion.

The model validation recorded a good agreement (Kappa = 0.78) and an overall accuracy of 90%.

The study provides valuable information that may help land-use planners, policy makers, and decision-makers on soil conservation practices for the area.

Compliance with ethical standards

Acknowledgments

The authors are grateful to the Ministry of Agricultural Development and Food Security for providing digital soil data, the Department of Meteorological Services (DMS) for availing climatic data, and the United States Geological Survey (USGS) Earth Resources Observation Systems (EROS) for downloading satellite images of the study area.

Disclosure of conflict of interest

We the authors hereby declare that there are no competing interests in this publication.

References

[1] Rahman MR, Shi ZH, Chongfa C. Soil erosion hazard evaluation-An integrated use of remote sensing, GIS and statistical approaches with biophysical parameters towards management strategies. Ecological Modelling. 2009; 220(13–14):1724–34.

[2] Snyman HA. Soil erosion and conservation. In: Tainton NM, ed. Veld Management in South Africa. Scottsville: University of Natal Press; 1999. p. 355-380.

[3] Department of Primary Industries [Internet]. Sydney: Department of Primary Industries; © 2014. Available from http://www.dpi.nsw.gov.au/agriculture /resources/s.

[4] Pimentel D, Burgess M. Soil erosion threatens food production. Agriculture (Switzerland). 2013; 3(3):443–463.

[5] Bai ZG, Dent DL, Olsson L, Schaepman ME. Proxy global assessment of land degradation. Soil Use & Management. 2008; 24:223–234.

[6] Manyiwa T, Dikinya O. Using universal soil loss equation and soil erodibility factor to assess soil erosion in Tshesebe village, North East Botswana. African Journal of Agricultural Research. 2013; 8(30):4170–78.

[7] Foster RH. Methods for assessing land degradation in Botswana. Earth & Environment. 2006; 1:238–276.

[8] Zerihun M, Mohammedyasin MS, Sewnet D, Adem AA, Lakew M. Assessment of soil erosion using RUSLE, GIS and remote sensing in NW Ethiopia. Geoderma Regional. 2018; 12:83-90.

[9] Ganasri BP, Ramesh H. Assessment of soil erosion by RUSLE model using remote sensing and GIS - A case study of Nethravathi Basin. Geoscience Frontiers. 2016; 7(6):953–961.

[10] Smith HJ. Application of empirical soil loss models in southern Africa: a review. South African Journal of Plant and Soil. 1999; 16(3):158-163.

[11] Vargas R, Omuto C. Soil loss assessment in Malawi. Food and Agriculture Organization of the United Nations, UNDP-UNEP Poverty-Environment Initiative and Ministry of Agriculture, Irrigation and Water Development, Malawi; 2016.

[12] Chen Y, Yu J, Khan S. Spatial sensitivity analysis of multi-criteria weights in GIS-based land suitability evaluation. Environmental Modelling & Software. 2010; 25(12):1582-91.

[13] Huete AR, Jackson RD, Post DF. Spectral response of plant canopy with different soil backgrounds. Remote Sensing of Environment. 1985; 17:37-53.

[14] Roose EJ. Use of the Universal Soil Loss Equation to predict erosion in west Africa. In: Erosion prediction and control, Soil Conservation Society of America, Special Publication No. 21, pp. 60-74.

[15] Morgan RPC. Soil erosion and conservation. London: Blackwell; 1986.

[16] Hurni, H. Erosion productivity conservation systems in Ethiopia. Proceedings of 4th International Conference on Soil Conservation, Maracay, Venezuela, 3-9 November 1985, 654-674.

[17] Kidane M, Bezie A, Kesete N, Tolessa T. The impact of land use and land cover (LULC) dynamics on soil erosion and sediment yield in Ethiopia. Heliyon. 2019; 5(12).

[18] Wischmeier WH, Smith DD. Predicting rainfall erosion losses: a guide to conservation planning. USDA Handbook No.537: USDA; 1978.

[19] Moisa MB, Negash DA, Merga BB, Gemeda DO. Impact of land use and land cover change on soil erosion using Rusle Model And Gis: A Case of Temeji Watershed, Western Ethiopia. Available from: https://doi.org/10.21203/rs.3.rs-100340/v1

[20] Ganasri BP, Ramesh H. Assessment of soil erosion by RUSLE model using remote sensing and GIS - A case study of Nethravathi Basin. Geoscience Frontiers. 2016; 7(6):953–961.

[21] Feda H. (2018). Assessment of soil erosion by R and USLE Model using remote sensing and GIS techniques: A case study of Huluka Watershed, Central Ethiopia [MSc thesis]. Addis Ababa, Ethiopia: University of Addis Ababa; 2018.

[22] Marondedze AK, Schütt B. Assessment of soil erosion using the RUSLE model for the Epworth District of the Harare Metropolitan Province, Zimbabwe. Sustainability- MDPI. 2020; 12(20):1-24.

[23] Parece T, Campbell JB, McGee J. Remote sensing analysis in an ArcMap environment. 2nd ed. Independently published; 2017.

[24] Phinzi K. Spatio-temporal appraisal of water-borne erosion using optical remote sensing and GIS in the Umzintlava Catchment (T32E), Eastern Cape, South Africa [M.Sc. thesis]. KwaZulu Natal: University of KwaZulu Natal; 2018.

[25] Moesi MS, Kayombo B, Tsheko R, Setlhabi E. Assessment of soil erosion by SLEMSA model using remote sensing and GIS: A case study of Taung Watershed of Ramotswa Agricultural District in Botswana. Global Journal of Engineering and Technology Advances. 2023; 15(1): 8-18.

[26] Matlhodi B, Kenabatho PK, Parida BP, Maphanyane JG. Evaluating land use and land cover change in the Gaborone dam catchment, Botswana, from 1984-2015 using GIS and remote sensing. Sustainability-MDPI. 2019; 11(19),5174.